Published online October 27, 2005

6000–6010 Nucleic Acids Research, 2005, Vol. 33, No. 18
doi:10.1093/nar/gki897

Depletion of TDP 43 overrides the need for exonic and intronic splicing enhancers in the human apoA-II gene

Pablo Arrisi Mercado[1], Youhna M. Ayala[1], Maurizio Romano[1,2], Emanuele Buratti[1] and Francisco E. Baralle[1,*]

[1]International Centre for Genetic Engineering and Biotechnology, Padriciano 99, I-34012 Trieste, Italy and [2]Department of Physiology and Pathology, University of Trieste, Via A. Fleming 22, 34127 Trieste, Italy

Received August 2, 2005; Revised September 19, 2005; Accepted September 27, 2005

ABSTRACT

Exon 3 of the human apolipoprotein A-II (apoA-II) gene is efficiently included in the mRNA although its acceptor site is significantly weak because of a peculiar $(GU)_{16}$ tract instead of a canonical polypyrimidine tract within the intron 2/exon 3 junction. Our previous studies demonstrated that the SR proteins ASF/SF2 and SC35 bind specifically an exonic splicing enhancer (ESE) within exon 3 and promote exon 3 splicing. In the present study, we show that the ESE is necessary only in the proper context. In addition, we have characterized two novel sequences in the flanking introns that modulate apoA-II exon 3 splicing. There is a G-rich element in intron 2 that interacts with hnRNPH1 and inhibits exon 3 splicing. The second is a purine rich region in intron 3 that binds SRp40 and SRp55 and promotes exon 3 inclusion in mRNA. We have also found that the (GU) repeats in the apoA-II context bind the splicing factor TDP-43 and interfere with exon 3 definition. Significantly, blocking of TDP-43 expression by small interfering RNA overrides the need for all the other *cis*-acting elements making exon 3 inclusion constitutive even in the presence of disrupted exonic and intronic enhancers. Altogether, our results suggest that exonic and intronic enhancers have evolved to balance the negative effects of the two silencers located in intron 2 and hence rescue the constitutive exon 3 inclusion in apoA-II mRNA.

INTRODUCTION

The pre mRNA splicing process leading to the synthesis of mature mRNA takes place in the spliceosome, a complex of small ribonucleoprotein particles (snRNPs) and splicing factors and is finely modulated (1,2). *Cis*-acting elements that influence splice site selection include the 5′ and 3′ splice sites, the branch point sequence and the polypyrimidine tract. Beyond the above mentioned canonical *cis*-acting elements, accessory sequences, such as exonic splicing enhancers (ESEs), exonic splicing silencers (ESSs), intronic splicing enhancers (ISEs) and intronic splicing silencers (ISSs) are also important for the definition of an exon (3,4).

Recently, we have demonstrated the existence of an ESE within the third exon of the apolipoprotein A-II (apoA-II) gene that specifically binds the SR proteins ASF/SF2 and SC35. The mutagenesis of this element prevented the binding of these *trans*-acting elements and caused *in vivo* skipping of exon 3 (5). Moreover, overexpression of ASF/SF2 and SC35 improved exon 3 inclusion, further supporting the positive involvement of these factors in exon 3 definition. Mechanistically, the recruitment of ASF/SF2 and SC35 might be acting as part of a scaffold to allow the recognition of the 3′ splice site, whose polypyrimidine tract is weak because of the peculiar $(GU)_{16}$ stretch adjacent to the intron/exon junction, which previous functional studies have indicated as a controller of exon 3 splicing (5). In this paper we show that the $(GU)_{16}$ stretch in the apoA-II context also binds the TDP-43 protein, a splicing factor implicated in the CFTR exon 9 skipping through its interaction with the (GU) repeats located within the 3′ splice site of CFTR intron 8 (6). Thus, we have revisited the function of the (GU) tract in apoA-II intron 2 by demonstration that its interaction with TDP-43 has an inhibitory role for the splicing of apoA-II exon 3, similarly to what was observed for the splicing of CFTR exon 9. Moreover, we have characterized a novel negative *cis*-acting element within apoA-II IVS2 and a positive *cis*-acting element in IVS3 involved in the control of the apoA-II exon 3 splicing. Interestingly, RNA interference against TDP-43 abolishes the effects of both exonic and intronic enhancer disruption. This result seems to indicate that ESEs and ISEs in the human

*To whom correspondence should be addressed. Tel: +39 040 3757337; Fax: +39 040 3757361; Email: baralle@icgeb.org

apoAII gene have evolved to counteract the negative effect of TDP43 binding to the (GU) repeats.

MATERIALS AND METHODS

Constructs

The wild-type and A97T sets of the pcDNApoIVS2 and pcDNApoIVS3 constructs were generated throughout overlap PCR method using apoA-II gene and apoA-II cDNA as templates. All pApo constructs carrying deletions or point mutations were generated by site-directed mutagenesis using standard PCR conditions. The identity of all constructs was checked by a CEQ2000 sequencer (Beckman Coulter, Fullerton, CA) according to the manufacturer's instructions. Constructs PTBApo-wt and PTBApo-A97T as well as PTBApo-wt-ISEmut and PTBApo-A97T-ISEmut were generated as follows: the apoA-II exon 3 plus portions of both flanking introns 2 (174 nt) and 3 (116 nt) were PCR-amplified from pApo-wt and pApo-A97T, respectively, and filled in with DNA polymerase (Klenow). The fragment was then inserted in a modified version of the α-globin–fibronectin EDB minigene in which this alternatively spliced exon had been removed to generate a unique Nde I site which was subsequently filled in with DNA polymerase I (Klenow) treatment, making it suitable for the insertion of the exon and its flanking introns under study. Constructs carrying partial deletions of either intron 2 or intron 3 were prepared starting from templates pApo-wt and pApo-A97T. The deletions were performed by overlapping PCRs products obtained using suitable primers. Generation of constructs mg$(GU)_{16}$ and mgΔ(GU) for *in vitro* experiments was carried out amplifying from pApo-wt and Δ(gu) plasmids (5) with the following couple of primers: SXhoI (5′-cccgctcgagcactgttaccaacatgaagct-3′) and HindIII/SacII AS (5′-ttttccgcggaagcttctctgcgaattctaagcctaatctgccctaa-3′). Whereas generation of construct $(GU)_{16}$-Ex3 was performed with the primers: ApoAII-TG/Exon3–5′ (XhoI) (5′-cccgctcgagggacccagctgaaaagag-3′) and ApoAII-Exon3–3′ (SacII) (5′-ttttccgcggaagcttttggcctcggcctgaa-3′).

Transfections

The DNA used for transient transfections was prepared with JetStar purification kit (Genomed, GmbH, Löhne, Germany) following the manufacturer's instructions. Then, 3 μg of DNA construct was transfected in 3×10^5 human hepatocarcinoma Hep3B cells using Qiagen Effectene transfection reagents. Total RNA was extracted using RNAwiz reagent (Ambion, Austin, TX) and retro-transcribed with poly(dT) primer. To amplify only the messenger derived from the transfections, PCRs were carried out with primers Ex1–1221 S (5′-accaaggacagagacgctggct-3′) and Not/Cla rev (5′-tctggacactgcggccgcatcg-3′) for constructs derived from pApo gene system and with primers α (5′-caacttcactcctaagccactg-3′) and Bra (5′-gggtcaccaggaagttggttaaatca-3′) for constructs derived from the α-globin–fibronectin EDB minigene (PTB). The conditions used for the PCRs were the following: 94°C for 5 min for the initial denaturation, 94°C for 30 min, 60°C for 1 min, 72°C for 1.5 min for 35 cycles, and 72°C for 7 min for the final extension. The PCRs were optimized to be in the exponential phase of amplification. For the SR protein overexpression experiments, 2 μg of the constructs pApo-wt, pApo-ISE3m, pApoA97T or pApoA97T-ISE3m was cotransfected with 2 μg of SRp40 and SRp55 coding sequences cloned into pCG vector (a kind gift of Dr J. Caceres). The results of all the transfections are the representative of at least three independent experiments. In order to quantify the proportion of alternative splicing, the relative amount of exon 3 skipping was quantified by optical densitometry.

RNA electrophoretic mobility shift assay (EMSA) and UV-crosslinking of protein and RNA

In order to generate the two different versions of human apoA-II intron 3 ISE RNAs, EcoRI–SalI double digestion was carried out on the construct pApo-wt and pApo-wt-ISE mut and subsequently cloned in pBluescript (SK) plasmid digested with the same enzymes. Once linearized with EcoRI, the constructs were *in vitro* transcribed in the presence of [α-^{32} P]UTP for 60 min at 37°C and treated with DNase for the same period of time. For EMSA, the [α-^{32}P]UTP-labeled RNA probes (4–6 fmol) were incubated with 5.2 mM HEPES, pH 7.9, 1 mM $MgCl_2$, 0.8 mM magnesium acetate, 0.52 mM DTT, 3.8% glycerol, 0,75 mM ATP, 1 mM GTP, 0.5 μg/μl heparin and 30 μg of HeLa nuclear extract (4C Biotech, Seneffe, Belgium) in a final volume of 20 μl for 20 min at room temperature. Following the addition of 5 μl of 50% (v/v) glycerol and tracking dye, the complexes were resolved on a 4% polyacrylamide gel (ratio of 19:1 acrylamide/bisacrylamide) in 75 mM Tris–glycine buffer (75 mM Tris and 75 mM glycine) at 15–25 mA for 3–4 h at 4°C. The gels were dried and exposed to X-OMAT AR films for 1–3 h. The UV-crosslinking assay was performed by incubation of the [α-^{32}P]UTP-labeled RNA probes (1×10^6 c.p.m./incubation) with 20 μg of HeLa nuclear extract in 20 μl of final volume at 30°C for 15 min. Final binding conditions were 20 mM HEPES, pH 7.9, 72 mM KCl, 1.5 mM $MgCl_2$, 0.78 mM magnesium acetate, 0.52 mM DTT, 3.8% glycerol, 0.75 mM ATP, 1 mM GTP and heparin at a 5 μg/μl final concentration as a nonspecific competitor. In the competition experiments increasing amounts of cold RNA (the molar ratios of cold/labeled RNA were 3 and 6) was also added as a competitor 5 min before addition of the labeled RNAs. The samples were then transferred in the wells of an HLA plate (Intermed, Nunc, Roskilde, Denmark) and irradiated with UV light on ice (800 000 kJ for 5 min). Unbound RNA was then digested with 30 μg of RNase A and 6 U of RNase T1 (Sigma) by incubation at 37°C for 30 min. The samples were then analyzed by 10% SDS–PAGE followed by autoradiography.

Crosslinking of RNA to adipic dehydrazide-agarose beads

Two synthetic RNA oligos IVS2-G123w, auaccuuuuuggggaggggcagagagc, and IVS2n-G123m, auaccuuuuugcggagcgcgcagagagc (Dharmacon, Chicago, IL), were generated and crosslinked to adipic dehydrazide–agarose beads. Afterwards they were separately incubated with HeLa nuclear extract with the addition of heparin to a final concentration of 5 μg/μl. Proteins were separated on a 10% SDS–PAGE gel and

visualized by Coomassie brilliant blue staining or electroblotted onto a nitrocellulose membrane and probed with a rabbit polyclonal anti-hnRNPH antiserum. Immunoblottings were detected using the ECL chemiluminescence kit (Pierce, Rockford, IL).

Immunoprecipitation of SR proteins and TDP-43 following UV-crosslinking

The UV-crosslinking of labeled RNAs with commercial HeLa nuclear extract was performed as described above. After the 30 min incubation with RNase at 37°C, 150 µl of immunoprecipitation (IP) buffer (20 mM Tris, pH 8.0, 300 mM NaCl, 1 mM EDTA and 0.25% Nonidet P-40) was added to each sample together with 1 µg of monoclonal antibodies mouse anti-SR 1H4 (Zymed Laboratories Inc., San Francisco, CA) and incubated for 2 h at 4°C on a rotator wheel. Afterward, 30 µl of protein A7G-Plus-agarose (Santa Cruz Biotechnology, Santa Cruz, CA) was added to each sample and incubated overnight at 4°C. The beads were subjected to four washing cycles with 1.5 ml of IP buffer and loaded on a 10% SDS–PAGE. The gels were run at a constant rate of 30 mA for 3.5 h, dried and exposed for 4–6 days with a Biomax Screen (Kodak, Rochester, NY). The [α-^{32}P]UTP-labeled RNA probes mg$(GU)_{16}$, mgΔ(GU) and $(GU)_{16}$-Ex3 used for UV-cross linking/IP were treated as described above, with the only difference that 1 µg of polyclonal antiserum against TDP-43 was added. After a 2 h incubation, 30 µl of Protein A/G-Plus Agarose (Santa Cruz Biotechnologies) was added to each sample and the mixture was incubated at 4°C overnight. The beads were then subjected to four washing cycles with 1.5 ml of IP buffer and loaded onto an SDS–PAGE. Gels were run at a constant 30 mA for ~3.5 h, dried, and then exposed for 4–6 days with a BioMax Screen (Kodak). Three independent IP assays were carried out for each antibody.

RNA interference against TDP-43

Hep3B cells (2×10^5) were seeded 24 h before the first transfection with the small interfering RNA (siRNA) oligonucleotide specific for TDP-43 (Y. M. Ayala, personal communication). Oligofectamine (3 µl) (Invitrogen BV, Leek, The Netherlands) was combined with 13 µl of Optimem medium (Invitrogen) and incubated for 7 min at room temperature (RT) (reaction 1). Meanwhile, in a different tube, 2.5 µl of the TDP-43 siRNA was mixed with 180 µl of Optimem (reaction 2). After the incubation, both reactions were mixed and left for 20 min at RT. Afterwards, the mix was added to the cells and maintained in the incubator at 37°C and 6% of CO_2 for 48 h. The cells were then washed with phosphate-buffered saline (PBS) and the transfection procedure was repeated with the difference that cells were maintained for only 24 h. Cells were washed with PBS and transfected with 0.5 µg of each minigene using Qiagen Effectene transfection reagents. RNA extraction and RT–PCR analysis were performed using primers complementary to sequences in the flanking fibronectin exonic sequences. Cell lysates were collected and analyzed for hnRNP H1 endogenous protein expression by western analysis using anti-H1 rabbit serum.

RESULTS

An intronic splicing enhancer is present within apoA-II intron 3

Our previous studies have evidenced that (i) the 3′ splice site of IVS2 is weak because of the (GU) tract adjacent to the acceptor site and (ii) a positive splicing *cis*-acting element (ESEwt) is placed within exon 3 and its alteration by point mutations (ESE-A97T) causes exon 3 skipping (5). In general, the interplay among different exonic and/or intronic sequences and the *trans*-acting factors can influence the recruitment of the constitutive splicing factors U2AF65 and U1 to the 3′ and 5′ splice site, respectively. We were interested to identify other apoA-II exon 3 splicing control elements eventually placed within its intronic flanking regions and to test these potential *cis*-acting elements in an heterologous system. For this purpose, the wild-type and A97T ApoA-II exon 3 (133 nt) with its flanking intronic regions (174 nt of intron 2 and 116 nt of intron 3) were cloned into the third intron of the pTB vector, which is an α-globin/fibronectin reporter minigene system used to study alternative splicing of several exons (7,8). (Figure 1A). The splicing profile from pTB minigenes overlapped those obtained with the pApo constructs (Figure 1B). In fact, pTBApo-wt and pTBApo-A97T constructs yielded 5 and 85% of exon 3 exclusion (Figure 1B, lanes 3 and 4), so mimicking substantially the splicing ratio from the corresponding variants in apoAII gene context (Figure 1B, lanes 1 and 2). These results indicate that the 423 nt genomic fragment of apoAII gene contains all the features important for efficient exon 3 inclusion in apoAII mRNA. Therefore, the pTB constructs can be used to the following mapping of potential intronic *cis*-acting elements that influence exon 3 splicing.

Initially, in order to verify the eventual presence of other apoA-II exon 3 splicing control elements, we screened its intronic flanking regions looking for possible *cis*-acting elements whose sequence might resemble previously described modulators of splicing. In order to look for other splicing control elements in IVS3, we created a deletion of 97 nt in intron 3 (from nt 1925 to 2022 in the apoA-II gene; GenBank accession number X04898.1) so obtaining the construct pApo-wt-Δ1925–2022 (Figure 1C). This 97 nt-deletion caused a 40% skipping of the exon 3 (Figure 1E, lane 3). This observation supports the existence of one or more elements within intron 3 that promote the inclusion of the apoA-II exon 3. We noticed the presence of three G runs in intron 3 just 10 bp downstream of the exon 3 donor splice site, namely I3G1 to I3G3, and a polypurine-rich sequence between nt 1935 and 1960 (Figure 1C). As these elements are close to the splice sites of exon 3, we have explored first the possible effects of G runs on the control of the apoA-II exon 3 splicing. To this aim, we first created mutants where the third, the first two and all the three G runs were disrupted by point mutations in intron 3. However, the transient transfection of this mutant did not show significant changes in the apoA-II exon 3 splicing pattern in comparison with the pApo-wt construct (Figure 1D). Thus, it is reasonable to exclude a role in the splicing of exon 3 for the G runs within intron 3. Conversely, the deletion of the purine-rich tract caused 25% apoA-II exon 3 skipping (Figure 1E, lane 4). In order to confirm the enhancing activity within nt 1941–1967, the continuity of the purine

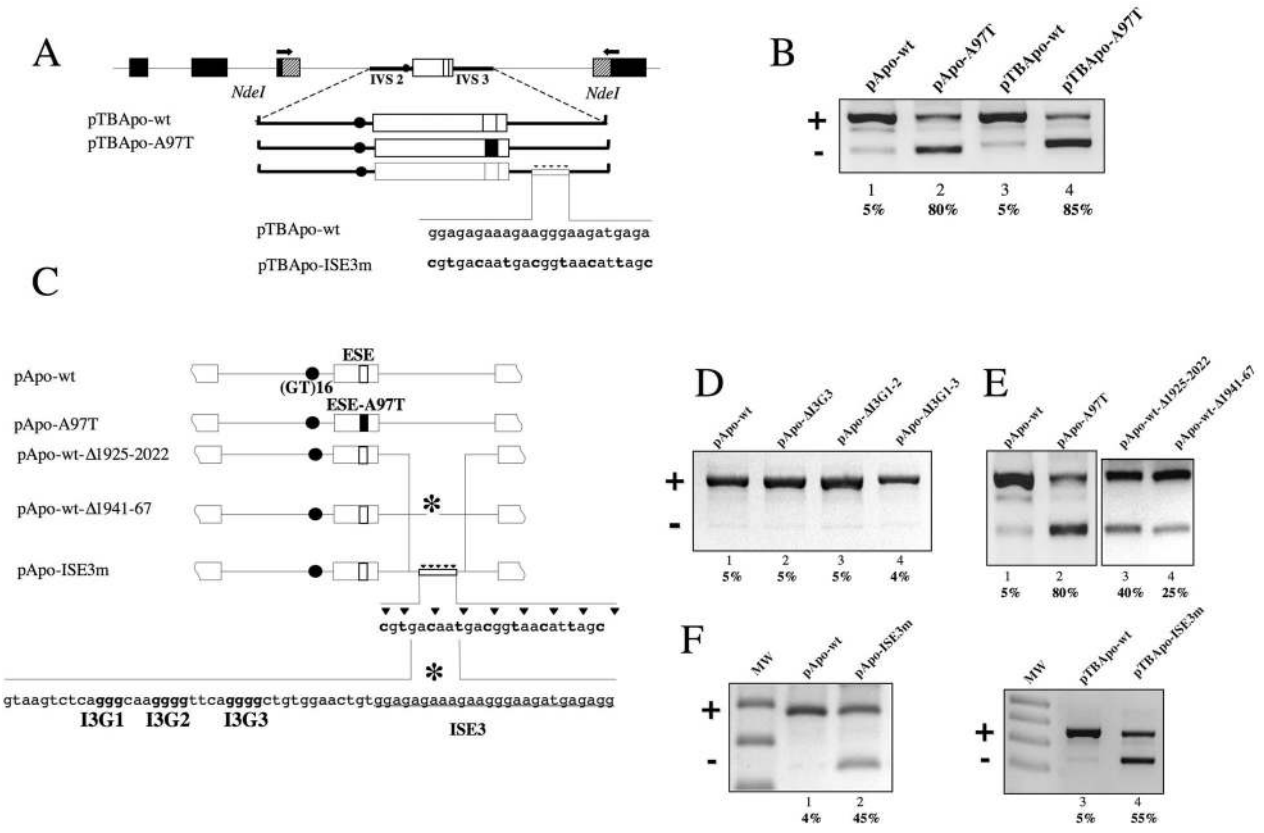

Figure 1. An ISE sequence is located within the human apoA-II intron 3. (**A**) Schematic representation of the α-globin/fibronectin reporter system (pTB) used to test the effect of the mutation in the apoA-II exon 3 ESE in a heterologous system α-globin, fibronectin EDB exons and human apoA-II exon 3 are indicated in black, shaded and white boxes, respectively. The black circle indicates the $(GT)_{16}$ tract. The superimposed arrows indicate the primers used in RT–PCR. The identity of the band is indicated at the left side of the gel. (**B**) Splicing pattern analysis of the RT–PCR products derived from cellular RNA, stained by ethidium bromide and separated on a 2% agarose gel. Comparison of the effect of the mutation A97T in the apoA-II exon 3 ESE when located in the pApo gene system and in the heterologous α-globin/fibronectin reporter system (pTB). (**C**) Schematic representation of the constructs carrying deletion and point mutations in the human apoA-II intron 3. White boxes, thin lines and the black circle represent the human apoA-II exons and introns and the $(GT)_{16}$ tract, respectively. The ESEwt and ESEA97T are indicated as small white and black boxes within the apoA-II exon 3, respectively. Part of the human apoA-II intron 3 sequences. The G runs are in bold. The asterisk indicates a 26 bp poly-purine rich region (underlined) deletion in the apoA-II intron 3. Arrowheads indicate the different point mutations within the polypurine region in intron 3. (**D**) Splicing pattern analysis by ethidium bromide staining of a 2% agarose gel electrophoresis of the RT–PCR product derived from cellular RNA. The disruption of the G runs in IVS3 was carried out as followed: in the construct pApo-ΔI3G3 ggggctg→gcttatg, in pApo-ΔI3G1–2 gggcaagggg→tcacaagcgc, and in pApo-ΔI3G1–3 gggcaaggggttcagggg→tgtcaagcattcatgcg. (**E**) Splicing pattern analysis of Hep3B transfected cells with constructs in which partial deletion of the intron 3 were carried out. (D) Schematic representation of the human apoA-II exon 3 and its flanking introns cloned in the α-globin/fibronectin reporter system (pTB). α-globin, fibronectin EDB exons and human apoA-II exon 3 are indicated in black, shaded and white boxes, respectively. The black circle indicates the $(GT)_{16}$ tract. The small white box within the exon 3 and the white rectangle in the intron 3 represents the ESE and the ISE, respectively. Arrowheads indicate the different point mutations within the polypurine region in intron 3. (**F**) Comparison of the splicing profiles produced by the mutations in the ISE both in the pApo gene system context and in the pTB reporter minigene. Relative amounts of exon 3 skipping are indicated below the lane numbers. The variability among three different experiments was always <20%.

stretch was disrupted by site-directed mutagenesis in the apoA-II gene and in the pTBApo contexts. Thus, constructs pApo-ISE3m and pTBApo-ISE3m were generated (Figure 1A and C, respectively). Point mutations within the potential ISE placed in intron 3 caused 45% exon 3 skipping in the pApo context and 55% exon 3 skipping in the pTBApo context (Figure 1F, lanes 2 and 4, respectively). Thus, consistently with the data obtained by the deletion, the results of point mutations confirmed the positive role for the polypurine element (ISE3) independently from the context.

SRp40 and SRp55 overexpression enhances splicing of apoA-II exon 3

Once verified the presence of a putative intronic splicing enhancer within intron 3 (ISE3), we were interested in identifying *trans*-acting factors possibly binding this region. As a first approach, EMSA was carried out by using two *in vitro* transcribed RNAs carrying either the ISE3wt or the ISE3 disrupted by the point mutation (ISE3m) (Figure 2A). The analysis showed two bands of shifted material with the transcript carrying the ISE3wt (upper complex, Uc, and lower complex, Lc) and only one band with ISE3m RNA (Figure 2B, compare lanes 3 and 4). A possible explanation for the difference in the number and mobility of the RNA–protein complexes might be the assembly of different factor/s upon ISE3wt and ISE3m RNAs.

The purine-rich content of ISE3 was reminiscent of exonic enhancer sequences, in fact ESE finder prediction of putative SR protein binding sites (9) showed the presence within the ISE of a high score site for SRp40 (data not shown). Total UV-crosslinking profiles did not show additional differences

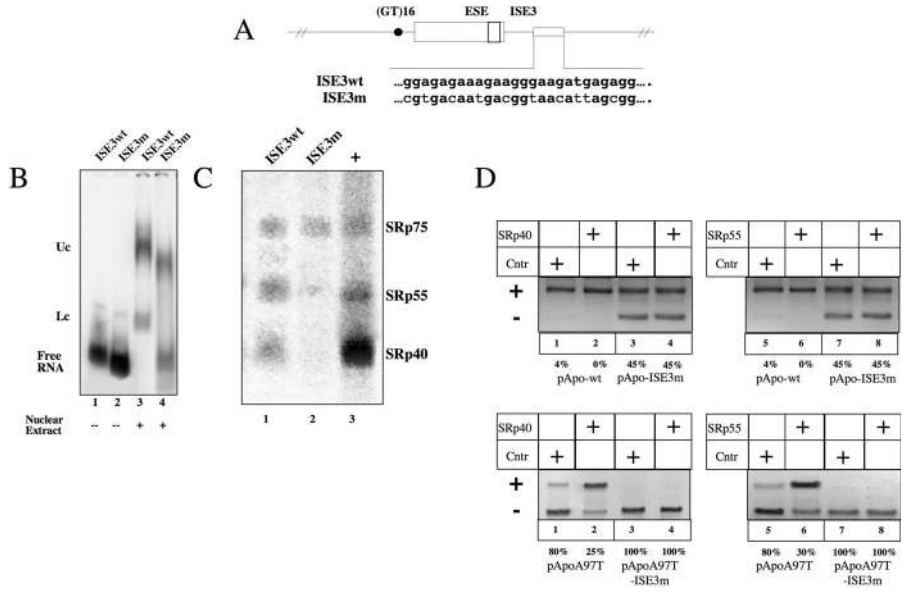

Figure 2. SRp40 and SRp55 interact with ISE-3 sequence and enhance splicing of exon 3. (**A**) Schematic representation of the constructs carrying wild-type (ISE3wt) and disrupted (ISE3m) ISE of apoA-II intron 3 used for the EMSA. (**B**) EMSA of ISE3wt and ISE3m RNAs incubated with HeLa nuclear extract. Complexes were then fractionated on a 4% non-denaturing polyacrylamide gel. The position of RNA–protein complexes (upper complex—Uc and lower complex—Lc) and free RNA are shown. Addition of nuclear extract is also indicated below the lane numbers (**C**) SDS–PAGE analysis of immunoprecipitation with the specific monoclonal antibody against the phosphorylated RS domain (MAb 1H4) following UV-crosslinking of the labeled RNAs ISE3wt, ISE3m and htot as a positive control (plus) (31). Specific immunoprecipitation of SRp40 (upper panel) and SRp55 (lower panel) is shown only with ISE3wt and htot RNAs. (**D**) Effects of SRp40 and SRp55 overexpression on apoA-II exon 3 splicing. Relative amounts of exon 3 skipping are indicated below the lane numbers. The variability among three different experiments was always <20%.

(data not shown). Therefore, in order to test the possible recruitment of SR proteins by the ISE3wt and ISE3m transcripts, we carried out UV-crosslinking analysis followed by immunoprecipitation using the monoclonal antibody 1H4 (mAb1H4), that recognizes mainly the phosphorylated domain of SRp40, SRp55 and SRp75 (10). The results showed that the ISE3wt but not the ISE3m RNA was able to immunoprecipitate both SRp40 and SRp55 (Figure 2C). Afterward, to test functionally the putative positive effects of SRp40 and SRp55, two pTBApo constructs carrying both the ESE in exon 3 and the ISE3 mutated were generated. Then, plasmids capable to express these SR proteins were cotransfected first along with pApo-wt and pApo-ISE3m. Figure 2D shows that cotransfection of pApo-wt with both SRp40 and SRp55 promoted full exon 3 inclusion (upper panel, lanes 2 and 6) when compared with the cotransfections with the control vector (upper panel, lanes 1 and 5). However, the overexpression of SRp40 and SRp55 with the construct carrying the ISE3m point mutation showed no significant variation in exon 3 inclusion levels (upper panel, lanes 4 and 8). In order to highlight better the effects of SR proteins overexpression, we repeated the cotransfection experiments with pApo-A97T and pApoA97T-ISE3m constructs. Because of the disruption of the ESE within exon 3, the basal level of exon 3 exclusion is higher and the effects of SR proteins are more detectable. However, the positive effects of the overexpression of SRp40 and SRp55 should cause an increase of exon 3 inclusion because the ISE3 element is intact. Consistently with this prediction, the lower panel of Figure 2D shows that the cotransfection of pApoA97T with SRp40 (lane 2) and SRp55 (lane 6) promoted exon 3 inclusion. Conversely, no variation in the levels of exon 3 inclusion was observed when the construct carrying the mutated ISE was cotransfected (lanes 4 and 8). Altogether these results indicate that both SRp40 and SRp55 interact with the sequence named ISE3 and have a functionally positive effect on apoA-II exon 3 inclusion.

A G-rich element with context-dependent functions is localized within apoA-II intron 2 and binds hnRNP-H1

Analysis of the sequences upstream of the polypyrimidine tract (GU repeated sequence) of exon 3 showed a region between nt 1639 and 1666 composed of four G runs (namely I2G1, I2G2, I2G3 and I2G4) (Figure 3A). Therefore, to test if these elements could affect the splicing of apoA-II exon 3, site-directed mutagenesis was carried out in these elements by disrupting the single G runs using pApo A97T as template. Figure 3B shows that the disruption of single I2G1 or I2G2 run rescued >90% of exon 3 inclusion, whereas mutagenesis of G3 run rescued ~60% of exon 3 inclusion (lanes 2–4, respectively). Conversely, the disruption of G4 as well as of T run immediately upstream of the G1 did not modify the splicing pattern of the pApo-A97T construct (lanes 5 and 6, respectively). Thus, these data suggest that G1, G2 and G3 runs have a negative effect on exon 3 inclusion in the apoA-II context. To confirm the role of these elements in apoA-II exon 3 splicing, we tested the effects of G runs mutagenesis also in the pTBApo context (Figure 3D). Surprisingly, the disruption of I2G1 and I2G2 runs caused >90% of exon 3 skipping (Figure 3D, lanes 2 and 3). However, the mutagenesis of

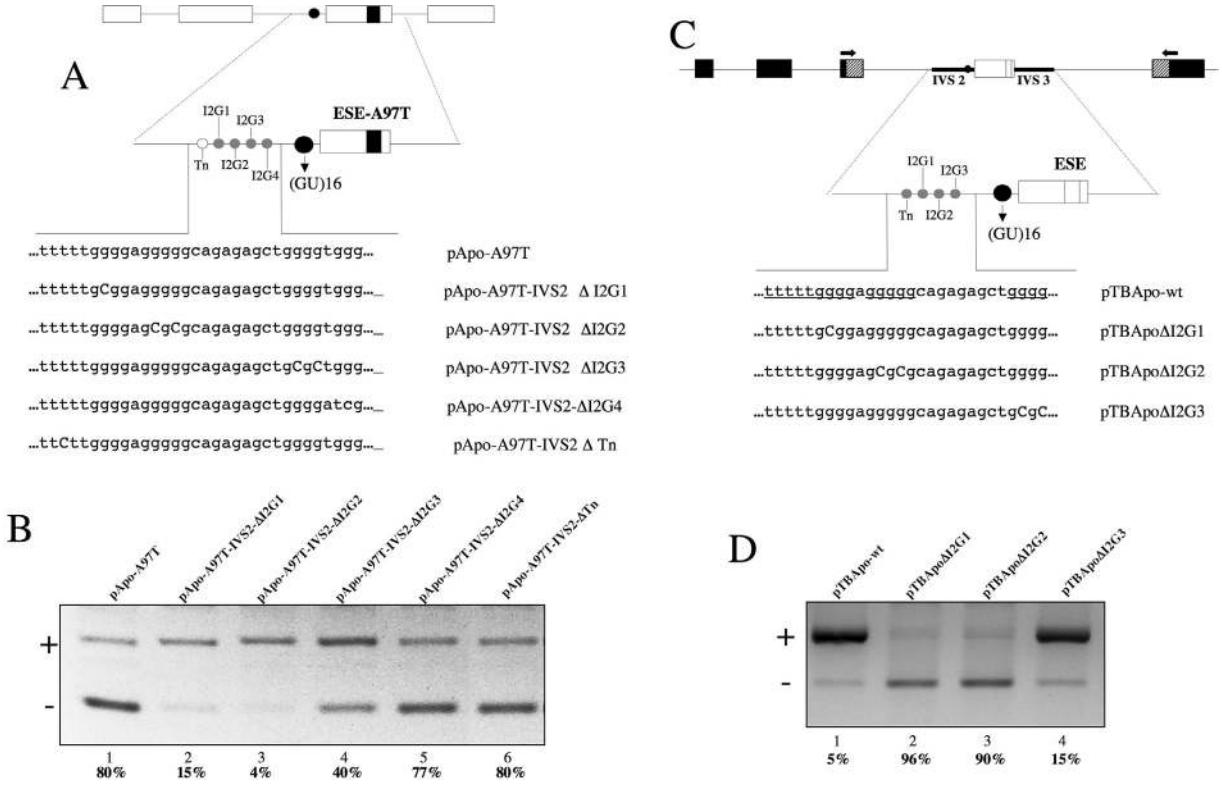

Figure 3. A G-rich sequence within the human apoA-II intron 2 influences exon 3 splicing according to context. (**A**) Schematic representation of the different constructs carrying point mutations in a regulatory sequence within the intron 2 in the pApo gene context. White boxes, thin lines and the black circle represent the human apoA-II exons, introns and the $(GT)_{16}$ tract, respectively. The ESEA97T is indicated as small black box within the apoA-II exon 3. Sequences within the apoA-II intron 2 changed by site-directed mutagenesis are indicated by small, white and gray circles. Partial sequence of the different constructs carrying point mutations in the intron 2 used for transfection in Hep3B cell line. (**B**) Agarose gel electrophoresis of RT–PCR products derived from constructs with single G runs or T run disruption in the pApo context. (**C**) Schematic representation of the different constructs carrying point mutations within the intron 2 of the apoA-II in pTB context. α-globin, fibronectin EDB exons and human apoA-II exon 3 are indicated in black, shaded and white boxes, respectively. Solid black lines, white box and black circle represent the human apoA-II introns, exon 3 and the $(GT)_{16}$ tract, respectively. The ESEwt is represented by a small white box inside the exon 3. Mutated nucleotides within the apoA-II intron 2 are indicated by small white and gray circles. Partial sequence of the different constructs carrying disrupting point mutations within intron 2. (**D**) Splicing pattern analysis by ethidium bromide staining of a 2% agarose gel electrophoresis of the RT–PCR products derived from constructs carrying single G run disruption in the pTB context. Relative amounts of exon 3 skipping are indicated below the lane numbers. The variability among three different experiments was always <20%.

I2G3 run did not show a significant variation of the pTBApowt splicing pattern (Figure 3D, lane 4). Therefore, the function of at least I2G1 and I2G2 runs in pTBApo do not mimic that in the pApo context. In fact, in the apoA-II gene context, they behave like an ISS, whereas in the pTBApo framework they behave like an ISE. This result underscores the importance of evaluating potential controlling regions in more than one minigene system. Nonetheless, in order to identify the *trans*-acting factors binding the G runs in the apoA-II intron 2 context, a pull-down assay was performed with synthetic RNA oligonucleotides containing either the I2G1 and I2G2 runs or the same sequence carrying point mutations within them (Figure 4A). This involved the crosslinking of transcribed IVS2-G12w and IVS2n-G12m RNAs to adipic acid dehydrazide agarose beads. Both beads preparations were separately incubated with HeLa nuclear extracts and the proteins bound were separated on an SDS–PAGE gel and then analyzed by Coomassie blue staining. Figure 4B shows a prominent band of ∼58 kDa molecular weight that could be observed only with the IVS2-G12w RNA containing the intact G runs. Considering that hnRNP-H1 is a splicing factor able to bind G runs (11) a western blot analysis with a polyclonal antibody against this protein was carried out thus confirming that the 58 kDa protein band corresponds to hnRNP-H1 (Figure 4C).

TDP-43 binds to $(GU)_{16}$ repeats in apoA-II intron 2 and represses exon 3 splicing

Our previous studies showed that, in the context of apoA-II, the $(GU)_{16}$ repeats seem to be important for exon 3 splicing (5,12,13). However, we have also reported the identification of TDP-43 as a *trans*-acting factor able to interact with the (GU)m polymorphic repeat region upstream from the 3′ splice site of the human CFTR exon 9 (6). In that report, it was demonstrated that TDP-43 has an inhibitory effect on exon 9 inclusion in the CFTR mRNA (6). This observation led us to investigate the possible role of this factor in the control of the apoA-II exon 3 splicing. In order to confirm the binding of TDP-43 to the $(GU)_{16}$ tract of apoA-II intron 2, we prepared the construct mg$(GU)_{16}$ that contains exon 2 and exon 3 sequences, the whole flanking intron 2 as well as the 5′ splice

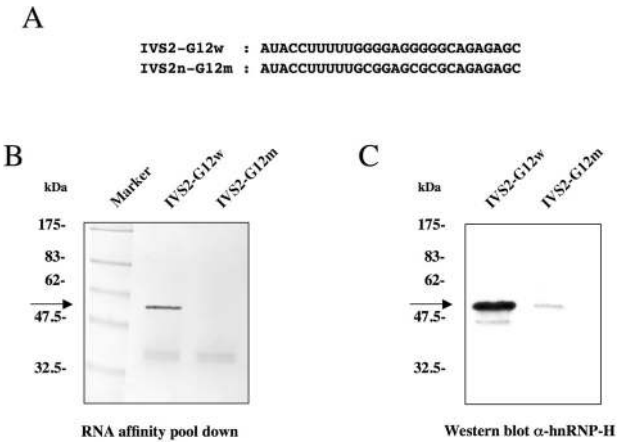

Figure 4. The hnRNPH1 binds to G runs within apoA-II intron 2. (**A**) Sequence of two synthetic RNA oligos carrying the wild-type or the disrupted G runs within the apoA-II intron 2 (IVS2-G12w and IVS2n-G12m, respectively). (**B**) The Coomassie stained gel of a pull-down assay using adipic dehydrazide beads derivatized with the RNAs following incubation with HeLa nuclear extract. In the lane from the IVS2-G12w-RNA-derivatized beads, the arrow indicates the 58 kDa protein that is absent in the IVS2n-G12m-RNA-derivatized beads. (**C**) Western blot analysis after the pull-down with the IVS2-G12w and IVS2n-G12m RNA oligos to determine the amount of hnRNPH1 binding.

site of intron 3 (Figure 5A). Moreover, two mutants where the whole GU repeated sequence was removed [mgΔ(GU)] or only a portion of IVS2 containing the GU tract with exon 3 and its 5′ splice site [(GU)16-Ex3] were also prepared (Figure 5A). These constructs were *in vitro* transcribed in the presence of [α-^{32}P]UTP and equal quantities of labeled transcripts were then used in a UV-crosslinking competition assay with HeLa nuclear extract. Figure 5B shows that, among the proteins that are crosslinked to the labeled mg$(GU)_{16}$ RNA, the band with the apparent molecular weight of 50 kDa was competed away only when increasing amount of cold $(GU)_{16}$-Ex3 RNA was added, but not when cold mgΔ(GU) was used as competitor (Figure 5B, compare lanes 1, 2 and 3 and 1, 4 and 5). Total competition was observed when the same mg$(GU)_{16}$ unlabeled RNA was added as control (Figure 5B).

In order to demonstrate that TDP-43 was the 50 kDa protein binding the GU repeats, immunoprecipitation experiments following the UV-crosslinking with a polyclonal antiserum against TDP-43 was carried out. Constructs mg$(GU)_{16}$ and mgΔ(GU) were *in vitro* transcribed in the presence of [α-^{32}P]UTP and equal amounts of labeled transcripts were then used in a UV-crosslinking assay with HeLa nuclear extract (data not shown). The UV-crosslinked samples were subsequently immunoprecipitated with a polyclonal antiserum against TDP-43 (6). Figure 5C shows that TDP-43 can be specifically immunoprecipitated by the anti-TDP-43 antiserum following UV-crosslinking with nuclear extract of a mg$(GU)_{16}$ RNA, but not from a mgΔ(GU) control RNA.

siRNA against TDP43 highlights the negative influence of this factor on apoA-II exon 3 splicing

In order to analyze the functional role that TDP-43 was playing in the apoA-II context, knock down of this protein was achieved through RNA-interference assay.

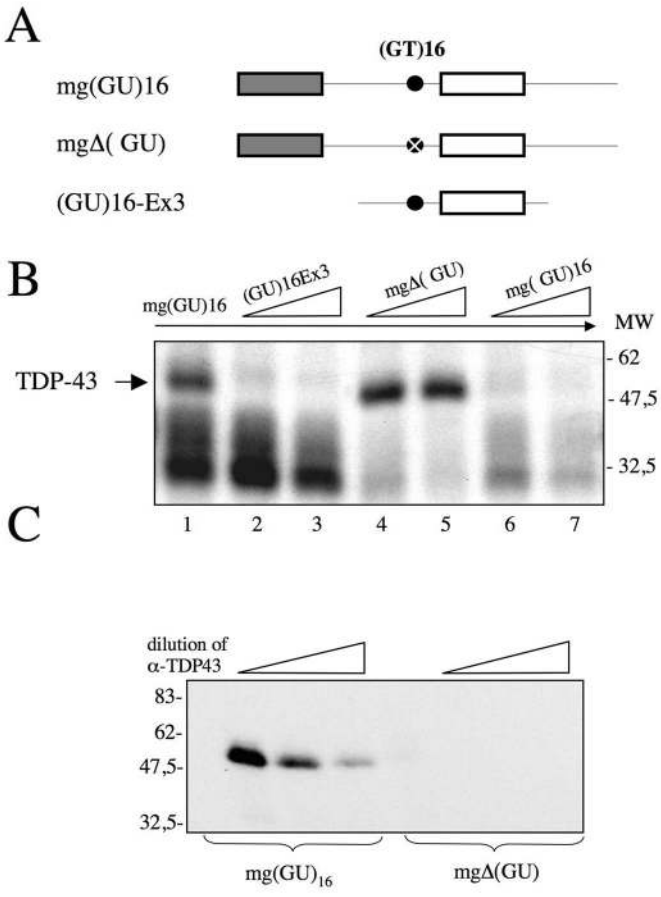

Figure 5. TDP-43 binds to the (GU) repeats in the apoA-II context. (**A**) Diagrammatic representation of minigene constructs used for competition experiments and immunoprecipitation with antibodies against TDP-43. Gray and white boxes represent the apoA-II exon 2 and 3, respectively. Thin lines and black circle correspond to the introns and the $(GT)_{16}$ repeats. Complete deletion of the $(GT)_{16}$ tract in the construct mgΔ(UG) is indicated by a white cross in the black circle. (**B**) UV-crosslinking with competition analysis following addition of 5- to 10-fold molar excess of cold $(GU)_{16}$-Ex3, mgΔ(GU) and mg$(GU)_{16}$ RNAs to labeled mg$(GU)_{16}$ RNA in the presence of HeLa nuclear extract. (**C**) UV-crosslinking plus immunoprecipitation with anti-TDP43 serum. [α-^{32}P]UTP-labeled mg$(GU)_{16}$ and mgΔ(GU) RNAs were incubated with HeLa nuclear extract before UV-crosslinking. Immunoprecipitation was then carried out with equal amounts of each UV-crosslinked sample using a polyclonal antiserum against TDP-43.

Double transfection of Hep3B cells at distance of 48 h with siRNA specific sequence for TDP-43 was carried out. After 24 h of the second transfection with the siRNA against TDP-43, constructs pApo-wt, pApo-A97T and pApo-ISE3m were transiently transfected in the TDP-43 knocked down Hep3B cells. Cell lysates were collected and analyzed for TDP-43 endogenous protein expression by western blot analysis using anti-TDP-43 rabbit serum. After normalization of total protein levels, we observed a strong reduction in the TDP-43 levels in Hep3B cells transfected with the TDP-43 siRNA, but not in untreated cells or in cells treated with a control siRNA (Figure 6A). Figure 6B shows the effects of TDP-43 silencing on splicing pattern analysis after RT–PCR. An increase in exon 3 inclusion was detected in cell transfected with pApo-wt and, more importantly, total rescue of exon 3 inclusion was observed in cells transfected with pApo-A97T

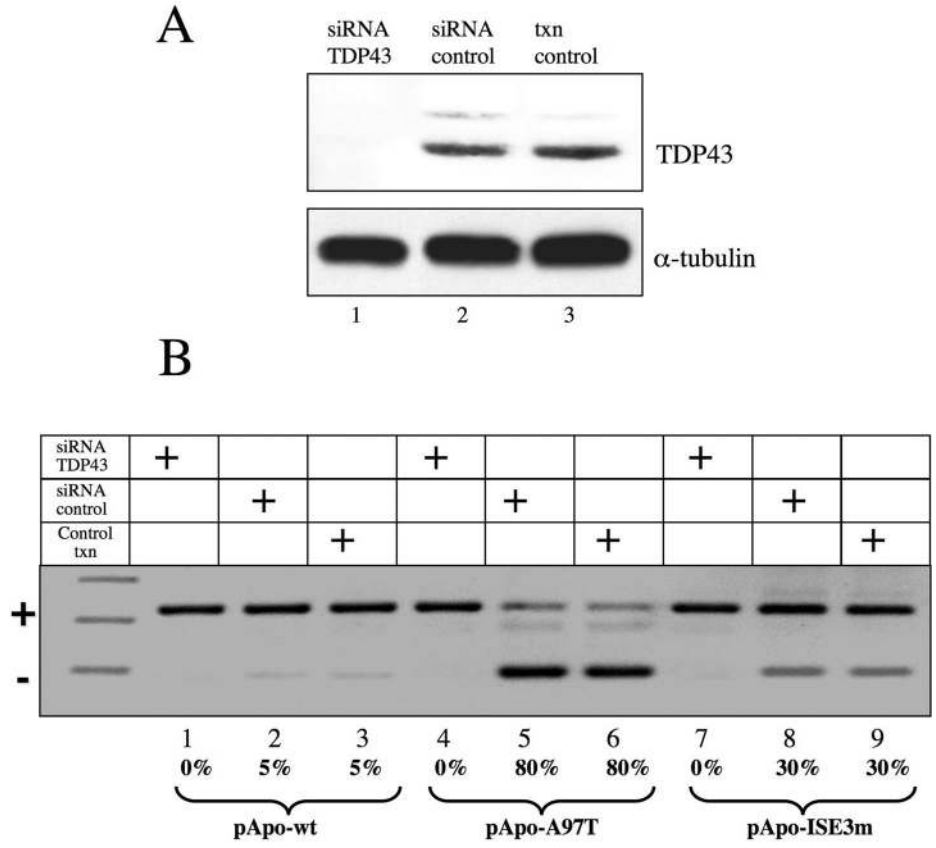

Figure 6. Knock down of TDP-43 causes the rescue of exon 3 inclusion. (**A**) Upper panel, western blot analysis of the cells treated with the siRNA oligonucleotide against TDP-43 (siRNA TDP43), control siRNA and mock transfected (lanes 1–3, respectively). TDP-43 expression was probed by western blot using a polyclonal antiserum. Lower panel, normalization control western blot with antibody against α-tubulin. (**B**) Shows splicing pattern analysis by ethidium bromide staining a 2% agarose gel of RT–PCR products after cotransfection of pApo-wt, pApo-A97T and pApo-ISE3m along with either the siRNA TDP43 (lanes 1, 4 and 7) or a control siRNA oligonucleotides (lanes 2, 5 and 8). The transfection of different variants of pApo gene system with no siRNA oligonucleotide was included as a control (lanes 3, 6 and 9).

and pApo-ISE3m (Figure 6B, compare lanes 4–5 and 7–8, respectively).

These results further support the observation that the interaction of TDP-43 with GU repeats has a negative effect on splicing of adjacent apoA-II exon 3, similarly to what has been observed in the CFTR exon 9 context (14). Moreover, these experiments highlight how the suppression of TDP-43 expression overrides the effect of disrupting the positive splicing controlling elements such as the enhancers placed in exon and intron 3.

DISCUSSION

Previous studies by our group have shown that human apoA-II exon 3 contains at least one ESE that is important to balance the low strength of its 3′ splice site (5). In this paper we considered that other elements, possibly located within flanking introns, might further contribute to the efficient splicing of exon 3.

A phylogenetic analysis of human apoA-II exon 3 and its flanking introns has evidenced that not only ESE sequence within exon 3 but also three other sequences are conserved in different species such as human, macaca, chimpanzee, mouse and rat with respect to the base composition and to the distance from the splice sites (Figure 7). The negative splicing element (GU) tract within intron 2 is conserved in chimpanzee (17 repeats) and *Macaca fascicularia* (7 repeats), whereas it is very short in rat (2 repeats) or absent in mouse. Interestingly, both the putative inhibitory G-rich element within intron 2 and the positive element within exon 3 are well conserved in all the species. Conversely, the ISE within intron 3 has a lower degree of homology in rodents (as compared with primate apoA-II genes). Therefore, these gene rearrangements might have placed negative *cis*-acting elements in proximity of the 3′ splice junction of apoA-II intron 2 and may have activated an evolutionary selection of different mechanism of splicing in order to improve the constitutive inclusion of apoA-II exon 3.

There are several splicing control elements located within introns (1,15). They can be involved in recognition of the appropriate splice site or in the suppression or enhancement of certain splice site usage, particularly in alternative splicing cases.

Relatively little is known about the nature of the intronic splicing controlling elements. Generally, they do not obey defined consensus rules and are known to consist of diverse sequences (16) although some common intronic *cis*-acting

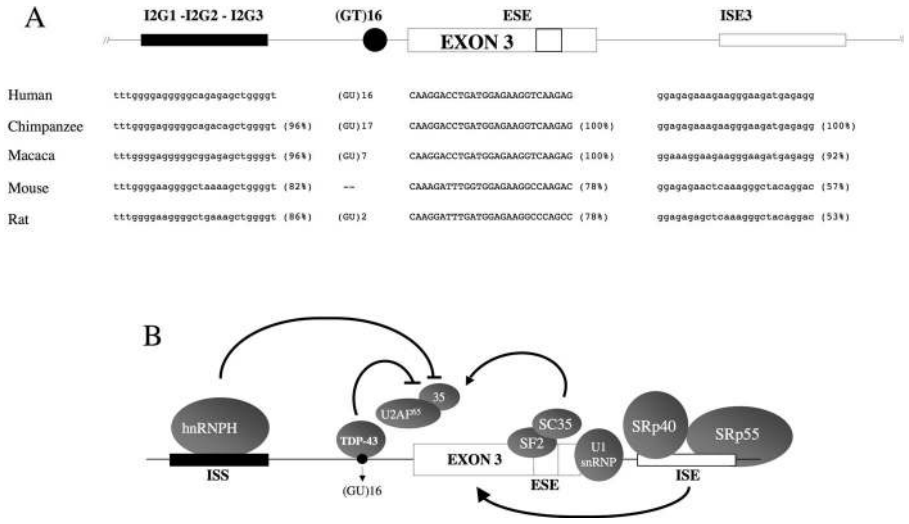

Figure 7. Evolutionary comparison of the regulatory elements found in human apoA-II exon 3 and its flanking introns in human, macaca, chimpanzee, mouse and rat. (**A**) Summary of the splicing control elements found in the human apoA-II gene. Black rectangle in intron 2, white square in the exon 3 and white rectangle in intron 3 represent the ISS, ESE and ISE *cis*-acting elements, respectively. Exon 3 is indicated, thin lines represent introns, and the black circle the $(GT)_{16}$ tract. The alignment of the different splicing control elements in different species is shown along with the percentage of identity in comparison with human sequences. (**B**) Cartoon showing a proposed model for the splicing mechanism of the apoA-II exon 3 splicing. TDP-43 and hnRNPH1 prevent the recruitment of U2AF65 to the 3′ splice site of apoA-II intron 2. ASF/SF2 and SC35 interacting with the ESE and SRp40 and SRp55 bound to the ISE might counteract this negative effect by forming a bridge-like structure among components bound to the 5′ and 3′ splice sites permitting the definition of exon 3.

elements have been observed, such as the GGG triplet (17–19), purine-rich sequences (20,21) or polypyrimidine tracts commonly present in the 3′ as well as 5′ regions of introns (22–24). It is known that the potential localization of intronic splicing *cis*-acting elements is extremely variable (20,25,26). We therefore considered the possible presence of splicing control elements in a range of 210 nt upstream of the exon 3 acceptor site and 116 nt downstream of the exon 3 donor site. The observation that the 26 nt-deletion of nt 1941–1967 in intron 3 causes exon 3 skipping strongly support the hypothesis that a sequence that positively controls the inclusion of exon 3 lies within that region. In a previous study, a purine-rich region (AGGAGAAGGGA) within the fibronectin EIIIB exon was found to interact with SRp40 (27). It was shown that this region is only partially responsible for stimulation of inclusion during SRp40 overexpression, and probably this protein acts at several different sites within the minigene. Interestingly, a sequence with a high degree of homology with the above described purine-rich region is present within the putative ISE3 within apoA-II intron 3 (AGAAGGGA). In addition, another study found that two GAR motifs are both required for stable interaction of SRp55 within the cardiac troponin T exon 5 (28). Moreover, it was noted that the binding of SRp55 to the target nucleotide sequence was efficient only when the whole cardiac troponin T exon 5 was present, suggesting that it can depend on RNA secondary structures. Indeed, in the apoA-II intron 3 context, the putative ISE-3 harbors a purine rich sequence. Therefore, the concomitant binding of SRp40 and SRp55 factors to the ISE3 region might occur, possibly by engaging other sequences outside the nt range 1941–1967 that spans the core of the ISE.

Previous studies on CFTR have shown that the interaction of SR proteins with intronic sequences inhibits the inclusion of the upstream proximal exon 9 in mRNA (7). However, there are other examples of ISEs that affect positively splicing of adjacent exons (29). The high contents of purines also might be indicative of a splicing control sequence since it seems to be the hallmark of these elements (3). In fact, we have demonstrated that the splicing factors SRp40 and SRp55 specifically bind the apoA-II transcript when ISE-3 is intact but not when it is mutagenized. Indeed, the positive involvement of SR proteins in apoA-II exon 3 splicing is supported by the fact that their overexpression improves exon 3 inclusion.

On the other side of exon 3, apoA-II intron 2 also seems to harbor different *cis*-acting elements involved in exon 3 splicing. Interestingly, we have identified a G-rich splicing control element whose activity is context-dependent: it has a silencer-like behavior within its natural apoA-II context, whereas it behaves like an enhancer-like element when placed in a heterologous context like that of fibronectin EDB. One possible explanation for this phenomenon is that the secondary structure of the G-rich region might change according to the context, so altering the accessibility of these sequences as demonstrated previously (30–32). In this work, we have shown that hnRNPH1 is one of the factors that bind to the G runs within apoA-II intron 2. Recent studies on the distribution of G runs within introns have shown that they enhance usage of proximal splice sites (18,33,34). Furthermore, splicing of the c-src N1 exon was shown to be mediated by an ISE located downstream of the N1 5′ splice site throughout interaction with hnRNP H (35). Conversely, other reports show that the G runs can have a silencer-like effect if placed within exons by binding to hnRNP H (19,36–38). It is apparent that our findings highlighted a G run-based *cis*-acting element within apoA-II intron 2 whose peculiarity is given not only by inhibiting splicing of the proximal downstream exon, but also by the observation that its function can change according to the intronic context where it is localized (Figure 3B

and D). In addition to a possible role of RNA structure, this context-dependent effect may also depend on interactions with the other splicing regulatory elements that are specific for the apoA-II gene. In addition, the enhancer/silencer activity might be affected by splicing events preceding the definition of apoA-II exon 3 or by the architecture of the transcriptional machinery (both constructs have different promoters) as demonstrated in other splicing models (39,40). Future studies will be aimed at characterizing the mechanisms of splicing control by G runs within IVS 2 and the role of hnRNP H1.

The other *cis*-acting element found close to the 3′ splice site of intron 2 consists in the $(GU)_{16}$ repeats that were previously shown to be functional as polypyrimidine tract (13). However, it is important the context where it is located: in fact, the replacement of the EDA exon polypyrimidine tract with the apoA-II $(GT)_{16}$ tract resulted in 95% of EDA exon exclusion (5). Furthermore, previous experiments on the apoA-II model showed that either the deletion of $(GU)_{16}$ tract or its replacement by $(CA)_{16}$ promoted exon 3 skipping (5,12). In principle, it could not be excluded that the deletion might cause exon 3 exclusion through alteration of branch point 3′ splice site spacing and that the replacement of $(GU)_{16}$ by $(CA)_{16}$ might interfere with the 3′ splice site definition because of the binding to another factor, such as hnRNP L that was recently described as able to bind to (CA) repeats in the eNOS gene (41). We now have confirmed that the apoA-II $(GU)_{16}$ repeats are bound specifically by TDP-43 protein, similarly to what happen in the CFTR intron 8 context (6). Considering that TDP-43 has a detrimental role for CFTR exon 9 splicing, we wondered if this factor might have a similar effect also in the apoA-II intron 2 context and that this effect was counteracted by the positive elements mapped above. Indeed, siRNA experiments to knock down TDP-43 in Hep3B cells have shown its inhibitory role also for apoA-II exon 3 splicing. This finding overlaps what was observed with CFTR exon 9, suggesting a general negative role of TDP-43 factors recruited by (GU) repeats placed at the 3′ splice site. Moreover, the observation that the (GU) tract do not bind to U2AF65 (13) suggest that different mechanisms for 3′ splice site recognition can exist. Altogether these observations further suggest that the 3′ splice site definition of the apoA-II exon 3 might be supported by other strong *cis*-acting elements that can contrast the negative effects of TDP-43 binding in proximity of the 3′ splice site of exon 3. The question arises if all these modulatory elements have evolved to counteract the negative influence of the weak 3′ splice site or have additional role in apoA-II splicing. The negative effect of TDP-43 on exon 3 splicing is remarkably more evident when we transfected the constructs pApo-A97T and pApo-ISE3m in cells where the expression of that protein was blocked by siRNA: in fact, TDP-43 silencing was able to fully rescue the effects of both exonic and intronic enhancer mutations. This finding suggests that apoA-II exon 3 definition can tolerate the disruption of splicing enhancers on condition that the inhibitory effects of TDP-43 is relieved. It follows that exon 3 splicing results from the coordinate action of positive *cis*-acting elements that balance the negative influence on apoA-II exon 3 splicing derived from the elements located at the 3′ end of intron 2. A large body of evidences indicates that U2AF35 is required for constitutive splicing and also works as a mediator of enhancer-dependent splicing (42). *In vitro* protein–RNA interaction studies with pre-mRNAs containing either a constitutive or regulated splicing enhancer have shown that U2AF35 directly mediates interactions between U2AF65 and proteins bound to the enhancers (43). On the basis of our data, in the apoA-II intron 2 context, without enhancers, U2AF65 should not work efficiently owing to the weakness of the polypyrimidine tract. We are temped to speculate that the interaction of TDP-43 with (GU) repeats and of hnRNPH1 to the G runs within intron 2 might interfere the function of U2AF65. Therefore, both the exonic and the intronic enhancers might have a pivotal role in definition of exon 3. However, the binding of ASF/SF2 and SC35 to the enhancer within exon 3 as well as the interaction of SRp40 and SRp55 to the sequence within intron 3 might be crucial to recruit the constitutive splicing factors U2AF35 and U2AF65 essential to define the 3′ splice site of intron 2. In this way, a bridge-like structure among components bound to the 5′ and 3′ splice sites would be formed to define exon 3 independently of the polypyrimidine tract pathway.

ACKNOWLEDGEMENTS

This work was supported by grants from Telethon Onlus Foundation—Italy (no. GGP02453) and F.I.R.B. (no. RBNE01W9PM) to F.E.B. Funding to pay the Open Access publication charges for this article was provided by ICGEB.

Conflict of interest statement. None declared.

REFERENCES

1. Smith,C.W. and Valcarcel,J. (2000) Alternative pre-mRNA splicing: the logic of combinatorial control. *Trends Biochem. Sci*., **25**, 381–388.
2. Black,D.L. (2003) Mechanisms of alternative pre-messenger RNA splicing. *Annu. Rev. Biochem*., **72**, 291–336.
3. Blencowe,B.J. (2000) Exonic splicing enhancers: mechanism of action, diversity and role in human genetic diseases. *Trends Biochem. Sci*., **25**, 106–110.
4. Hovhannisyan,R.H. and Carstens,R.P. (2005) A novel intronic *cis* element, ISE/ISS-3, regulates rat fibroblast growth factor receptor 2 splicing through activation of an upstream exon and repression of a downstream exon containing a noncanonical branch point sequence. *Mol. Cell. Biol*., **25**, 250–263.
5. Arrisi-Mercado,P., Romano,M., Muro,A.F. and Baralle,F.E. (2004) An exonic splicing enhancer offsets the atypical GU-rich 3′ splice site of human apolipoprotein A-II exon 3. *J. Biol. Chem*., **279**, 39331–39339.
6. Buratti,E., Dork,T., Zuccato,E., Pagani,F., Romano,M. and Baralle,F.E. (2001) Nuclear factor TDP-43 and SR proteins promote *in vitro* and *in vivo* CFTR exon 9 skipping. *EMBO J*., **20**, 1774–1784.
7. Pagani,F., Buratti,E., Stuani,C., Romano,M., Zuccato,E., Niksic,M., Giglio,L., Faraguna,D. and Baralle,F.E. (2000) Splicing factors induce CFTR exon 9 skipping through a non-evolutionary conserved intronic element. *J. Biol. Chem*., **275**, 21041–21047.
8. Buratti,E., Dork,T., Zuccato,E., Pagani,F., Romano,M. and Baralle,F.E. (2001) Nuclear factor TDP-43 and SR proteins promote *in vitro* and *in vivo* CFTR exon 9 skipping. *EMBO J*., **20**, 1774–1784.
9. Cartegni,L., Wang,J., Zhu,Z., Zhang,M.Q. and Krainer,A.R. (2003) ESEfinder: a web resource to identify exonic splicing enhancers. *Nucleic Acids Res*., **31**, 3568–3571.
10. Neugebauer,K.M. and Roth,M.B. (1997) Distribution of pre-mRNA splicing factors at sites of RNA polymerase ImI transcription. *Genes Dev*., **11**, 1148–1159.
11. Matunis,M.J., Xing,J. and Dreyfuss,G. (1994) The hnRNP F protein: unique primary structure, nucleic acid-binding properties, and subcellular localization. *Nucleic Acids Res*., **22**, 1059–1067.

12. Shelley,C.S. and Baralle,F.E. (1987) Deletion analysis of a unique 3′ splice site indicates that alternating guanine and thymine residues represent an efficient splicing signal. *Nucleic Acids Res*., **15**, 3787–3799.
13. Coolidge,C.J., Seely,R.J. and Patton,J.G. (1997) Functional analysis of the polypyrimidine tract in pre-mRNA splicing. *Nucleic Acids Res*., **25**, 888–896.
14. Buratti,E. and Baralle,F.E. (2001) Characterization and functional implications of the RNA binding properties of nuclear factor TDP-43, a novel splicing regulator of CFTR exon 9. *J. Biol. Chem*., **276**, 36337–36343.
15. Ladd,A.N. and Cooper,T.A. (2002) Finding signals that regulate alternative splicing in the post-genomic era. *Genome Biol*., **3**, reviews0008.
16. Fairbrother,W.G. and Chasin,L.A. (2000) Human genomic sequences that inhibit splicing. *Mol. Cell. Biol*., **20**, 6816–6825.
17. Carlo,T., Sterner,D.A. and Berget,S.M. (1996) An intron splicing enhancer containing a G-rich repeat facilitates inclusion of a vertebrate micro-exon. *RNA*, **2**, 342–353.
18. McCullough,A.J. and Berget,S.M. (1997) G triplets located throughout a class of small vertebrate introns enforce intron borders and regulate splice site selection. *Mol. Cell. Biol*., **17**, 4562–4571.
19. Romano,M., Marcucci,R., Buratti,E., Ayala,Y.M., Sebastio,G. and Baralle,F.E. (2002) Regulation of 3′ splice site selection in the 844ins68 polymorphism of the cystathionine b-synthase gene. *J. Biol. Chem*., **12**, 12.
20. McCullough,A.J. and Schuler,M.A. (1997) Intronic and exonic sequences modulate 5′ splice site selection in plant nuclei. *Nucleic Acids Res*., **25**, 1071–1077.
21. Hastings,M.L., Wilson,C.M. and Munroe,S.H. (2001) A purine-rich intronic element enhances alternative splicing of thyroid hormone receptor mRNA. *RNA*, **7**, 859–874.
22. Pagani,F., Buratti,E., Stuani,C., Bendix,R., Dork,T. and Baralle,F.E. (2002) A new type of mutation causes a splicing defect in ATM. *Nature Genet*., **30**, 426–429.
23. Zuccato,E., Buratti,E., Stuani,C., Baralle,F.E. and Pagani,F. (2004) An intronic polypyrimidine-rich element downstream of the donor site modulates cystic fibrosis transmembrane conductance regulator exon 9 alternative splicing. *J. Biol. Chem*., **279**, 16980–16988.
24. Hastings,M.L. and Krainer,A.R. (2001) Functions of SR proteins in the U12-dependent AT-AC pre-mRNA splicing pathway. *RNA*, **7**, 471–482.
25. Zheng,Z.M., Quintero,J., Reid,E.S., Gocke,C. and Baker,C.C. (2000) Optimization of a weak 3′ splice site counteracts the function of a bovine papillomavirus type 1 exonic splicing suppressor *in vitro* and *in vivo*. *J. Virol*., **74**, 5902–5910.
26. Rowen,L., Young,J., Birditt,B., Kaur,A., Madan,A., Philipps,D.L., Qin,S., Minx,P., Wilson,R.K., Hood,L. *et al*. (2002) Analysis of the human neurexin genes: alternative splicing and the generation of protein diversity. *Genomics*, **79**, 587–597.
27. Du,K., Peng,Y., Greenbaum,L.E., Haber,B.A. and Taub,R. (1997) HRS/SRp40-mediated inclusion of the fibronectin EIIIB exon, a possible cause of increased EIIIB expression in proliferating liver. *Mol. Cell. Biol*., **17**, 4096–4104.
28. Nagel,R.J., Lancaster,A.M. and Zahler,A.M. (1998) Specific binding of an exonic splicing enhancer by the pre-mRNA splicing factor SRp55. *RNA*, **4**, 11–23.
29. Gallego,M.E., Gattoni,R., Stevenin,J., Marie,J. and Expert-Bezancon,A. (1997) The SR splicing factors ASF/SF2 and SC35 have antagonistic effects on intronic enhancer-dependent splicing of the beta-tropomyosin alternative exon 6A. *EMBO J*., **16**, 1772–1784.
30. Buratti,E. and Baralle,F.E. (2004) Influence of RNA secondary structure on the pre-mRNA splicing process. *Mol. Cell. Biol*., **24**, 10505–10514.
31. Buratti,E., Muro,A.F., Giombi,M., Gherbassi,D., Iaconcig,A. and Baralle,F.E. (2004) RNA folding affects the recruitment of SR proteins by mouse and human polypurinic enhancer elements in the fibronectin EDA exon. *Mol. Cell. Biol*., **24**, 1387–1400.
32. Muro,A.F., Caputi,M., Pariyarath,R., Pagani,F., Buratti,E. and Baralle,F.E. (1999) Regulation of fibronectin EDA exon alternative splicing: possible role of RNA secondary structure for enhancer display. *Mol. Cell. Biol*., **19**, 2657–2671.
33. Sirand-Pugnet,P., Durosay,P., Brody,E. and Marie,J. (1995) An intronic (A/U)GGG repeat enhances the splicing of an alternative intron of the chicken beta-tropomyosin pre-mRNA. *Nucleic Acids Res*., **23**, 3501–3507.
34. McCullough,A.J. and Berget,S.M. (2000) An intronic splicing enhancer binds U1 snRNPs to enhance splicing and select 5′ splice sites. *Mol. Cell. Biol*., **20**, 9225–9235.
35. Chou,M.Y., Rooke,N., Turck,C.W. and Black,D.L. (1999) hnRNP H is a component of a splicing enhancer complex that activates a c-src alternative exon in neuronal cells. *Mol. Cell. Biol*., **19**, 69–77.
36. Chen,C.D., Kobayashi,R. and Helfman,D.M. (1999) Binding of hnRNP H to an exonic splicing silencer is involved in the regulation of alternative splicing of the rat beta-tropomyosin gene. *Genes Dev*., **13**, 593–606.
37. Jacquenet,S., Mereau,A., Bilodeau,P.S., Damier,L., Stoltzfus,C.M. and Branlant,C. (2001) A second exon splicing silencer within human immunodeficiency virus type 1 tat exon 2 represses splicing of Tat mRNA and binds protein hnRNP H. *J. Biol. Chem*., **276**, 40464–40475.
38. Pagani,F., Buratti,E., Stuani,C. and Baralle,F.E. (2003) Missense, nonsense, and neutral mutations define juxtaposed regulatory elements of splicing in cystic fibrosis transmembrane regulator exon 9. *J. Biol. Chem*., **278**, 26580–26588.
39. Cramer,P., Pesce,C.G., Baralle,F.E. and Kornblihtt,A.R. (1997) Functional association between promoter structure and transcript alternative splicing. *Proc. Natl Acad. Sci. USA*, **94**, 11456–11460.
40. Pagani,F., Stuani,C., Zuccato,E., Kornblihtt,A.R. and Baralle,F.E. (2003) Promoter architecture modulates CFTR exon 9 skipping. *J. Biol. Chem*., **278**, 1511–1517.
41. Hui,J., Stangl,K., Lane,W.S. and Bindereif,A. (2003) HnRNP L stimulates splicing of the eNOS gene by binding to variable-length CA repeats. *Nature Struct. Biol*., **10**, 33–37.
42. Graveley,B.R., Hertel,K.J. and Maniatis,T. (2001) The role of U2AF35 and U2AF65 in enhancer-dependent splicing. *RNA*, **7**, 806–818.
43. Zuo,P. and Maniatis,T. (1996) The splicing factor U2AF35 mediates critical protein-protein interactions in constitutive and enhancer-dependent splicing. *Genes Dev*., **10**, 1356–1368.